USE OF ACTIVE CONTROL TECHNOLOGY TO IMPROVE RIDE QUALITIES OF LARGE TRANSPORT AIRCRAFT

Gerald C. Cohen, Clifford J. Cotter, and Donald L. Taylor
Boeing Commercial Airplane Company

SUMMARY

This paper describes the analyses, construction and flight testing of two systems, "Beta-vane" and modal suppression augmentation system (MSAS), which were developed to suppress gust induced lateral accelerations of large aircraft. The Boeing 747 transport was used as the test vehicle. The purpose of the Beta-vane system is to reduce acceleration levels at the "dutch roll" frequency whereas the function of the MSAS system is to reduce accelerations due to flexible body motions caused by turbulence. Data from flight test, with both systems engaged shows a 50-70 percent reduction in lateral aft body acceleration levels. Furthermore, this paper suggests that present day techniques used for developing dynamic equations of motion in the flexible mode region are limited. These techniques produce results which are satisfactory for analyzing dynamic loads and stability problems, but may be insufficient for development of active control systems operating in the same frequency region.

INTRODUCTION

The aft fuselage section of long slender airplanes is a position of relatively high lateral acceleration levels in moderate to heavy turbulence. These accelerations can be considered as being due to contributions from a rigid airplane with the elastic effects superimposed. Initially, because of the experimental nature of the program, two different approaches to gust alleviation were undertaken. One system worked the flexible body frequencies (MSAS system - Section I) whereas the second system worked primarily rigid body frequencies (Beta-vane system - Section II).

SECTION I

MODAL SUPPRESSION AUGMENTATION SYSTEM (MSAS)

INTRODUCTION

This section of the paper will describe in detail the analysis, construction and flight testing of a modal suppression augmentation system. This system was designed to reduce aft body lateral accelerations in the 1-3 Hz region when flexible body motions are perturbed by turbulence. Due to the problems associated with the lateral dynamic equations of motions as discussed in the following section (that is,comparison of analytical and measured transfer functions showed a variation in the flexible mode region), a technique was developed which involved 'curve fitting' transfer functions to experimental data. This method then allowed a modal suppression system to be developed without dependence on the analytical equations. Furthermore, by including the yaw damper actuator with the experimental data that was analyzed via the curve fit method, the problem associated with precise mathematical modeling of the structural compliance feedback-actuator system was avoided.

COMPARISON OF ANALYTICAL AND EXPERIMENTAL DATA

Results from 747 flight testing in turbulence indicated that aft end lateral motion was composed of the following two components:

(1) Rigid Airplane (dutch roll) --- 0.2 Hz
(50% contribution)

(2) Elastic effects --- 1.0 - 3.0 Hz
(50% contribution)

Within the 1.0 - 3.0 Hz band of frequencies the analytical equations predict five free-free modes, all of which are composed to some degree of wing, nacelle and body motions. These modes (corrected with results from

the ground vibration test) are shown in Figure 1. Flight test data reduced via the 'curve fitting' technique (explained in the following section) is also shown in Figure 1.

Based on their composition the modes are identified as (1) outboard nacelle vertical bending, (2) fundamental wing bending, (3) inboard nacelle side bending, (4) aft body bending, and (5) outboard nacelle side bending. In addition to the above set of modes, a stabilizer mode at 3.16 Hz, a fore body mode at 4 Hz and a vertical fin bending mode at 6 Hz are of concern in conjunction with the development of the MSAS filter.

Although the analytical equations were reasonably close to measured values and thus sufficient for flutter studies, the development of an active control system, however, requires not only that the characteristic equation be correct but also that the residues of the transfer function (the zeros shown in Figure 1) be properly described.

From Figure 1, it is seen that even though the roots of the system (poles) are identified and reasonably close to those obtained via flight test data, it is obvious that the associated zeros are misaligned. Various attempts in the form of refinement in both structural and aerodynamic representation did not succeed in changing the general picture. Further work along these lines still remains to be pursued.

As a practical solution to the problem, a curve fitting technique was applied to the measured transfer-functions to identify the zeros and poles of the system to be controlled.

CURVE FITTING TECHNIQUE

From initial experimental data, the aft body was found to resonate at 1.8 and 2.4 Hz whereas the fundamental frequency of the fore body was 4 Hz. Furthermore, the aft body could be perturbed by gusts striking the fin or gusts exciting the engine nacelles producing wing-body coupling suggesting that either the ailerons or rudders could be used for the active control system. Due to the complexity associated with developing a system in conjunction with the ailerons, a rudder suppression

system was chosen. Though the command signal to the rudder is rate limited at 13 deg/sec compared to a 50 deg/sec requirement for the load alleviation system developed for the B-52, it was determined that this lower rate limit would satisfy the requirement.

The experimental data was obtained by excitation of the lateral airframe degrees of freedom in the 1-7 Hz region via the upper and lower yaw damper servos and their respective rudders. The forcing function itself was a continuously changing constant amplitude sine wave frequency sweep, in the 1-7 Hz range, which was produced on a computer and stored on magnetic tape. Using the experimental data in conjunction with a Fast Fourier transform data reduction package, Bode plots for various sensor locations on the aircraft could be obtained.

The curve fitting' technique is based on the 2 papers given in references 1 and 2. These algorithms were programmed on the CDC 6600 during the development of the Boeing SST and were used in the design of 3rd and 4th order prefilters in conjunction with the Horowitz Circle technique. After a few attempts at deriving transfer functions from the experimental data, the following deficiencies in the computer program were observed:

1. The program could not handle 14th order systems.

2. The small non-linearities associated with the amplitude and phase curves were sufficient to make the computer program limit cycle.

3. The program was very sensitive to end point conditions.

Transfer functions that matched the experimental data were obtained by incorporating the following procedures:

1. The transfer functions were assumed to be of minimum phase (no right half plane zeros). Therefore, only the amplitude was input to the program.

2. A pole or pole-zero combination is always included on either side of the band of frequencies that is of interest.

The transfer functions showed clearly that although the analytic equations could be manipulated so that the modes would have the correct frequencies, the zeros associated with these analytic equations (and therefore the phase) were not correct for the 2.1 and 2.4 Hz modes. The effects of the different zero locations on a control system will now be shown.

A root locus diagram of an accelerometer control system based on the analytical equations is shown in Figure 2. The control system adds approximately twice the damping to the 2nd and 4th modes; these two modes contribute 80% of the flexible energy. This system was flight tested and results showed that the 4th mode was destabilized and the 2nd mode increased in frequency as the gain of the control system was increased. This same control system based on the airplane transfer function obtained via the curve fit computer program has the root locus diagram shown in Figure 3. Notice that the loci are almost the same as those obtained in flight. This experimental verification of the curve fit technique showed that this method could be used with confidence.

The complete design technique in the development of the MSAS is the following:

1. EXCITE AIRPLANE VIA RUDDERS - CONSTANT AMPLITUDE SINE WAVE 1.0 to 7.0 HZ.

2. CURVE FIT TRANSFER FUNCTION TO AFT BODY SENSORS.

3. ROOT LOCUS METHODS TO DESIGN FILTER.

4. EXCITE AIRPLANE VIA RUDDERS, WITH/WITHOUT MSAS, TO VERIFY SUPPRESSION OF MODES.

5. FLY MSAS IN TURBULENCE TO VERIFY CONTROL SYSTEM.

Notice that this procedure does not allow analytical verification of gust suppression; it only substantiates analytically whether the control system adds damping to the modes.

Two control systems were designed and flight tested using the above procedure. The first system used an aft body mounted lateral accelerometer sensor whereas the second system used two yaw rate gyros, one aft body and one at the cg. Figure 4 shows the reduction in aft body acceleration (Body Station 2300) for the two systems when

the sine wave forcing function is fed to the lower rudder and the control systems are commanding the upper rudder. The accelerometer system was not chosen because the 2.4 Hz mode destabilized at high 'q' conditions. In addition, to obtain equal reduction in acceleration levels during turbulence, the accelerometer system required more rudder than the gyro system suggesting that the gust zeros for the two systems were quite different.

DESCRIPTION OF FINAL MSAS SYSTEM

The MSAS system is a single channel augmentation system working via the lower yaw damper servo. A block diagram of the control system is shown in Figure 5. The augmentation system provides damping to the 1.8, 2.1, and 2.4 Hz aft body lateral modes without disturbing the dutch roll mode. The salient features of the system are the following:

1. Two lateral yaw rate gyros.

2. Single channel 'real time' monitoring.

3. Scheduling of filter gain with calibrated air speed (CAS).

4. Output of system limited to + 0.8 degrees of rudder (yaw damper authority is $\pm$ 3.5 degrees of rudder).

5. Operation of system limited to flaps "up" condition.

Figure 6 represents a functional block diagram of the computational path.

1. MSAS Damping Signal

   The MSAS signal is derived from the subtraction of two yaw rate signals. The location of the sensors are the following:

   a. Aft End Gyro:

      Body Station 2280, WL190, RBL20

b. CG Gyro:

Body Station 1307, WL195, RBL5

Due to the placement, the aft end gyro is sensitive to dutch roll and flexible mode frequencies whereas the cg gyro is sensitive only to dutch roll frequencies. Upon subtraction of the two yaw rate signals, the remaining signal contains only flexible mode frequencies.

2. Band Pass Filter

At flaps up condition, the yaw rate signal passes through a band pass filter into the yaw damper servo amplifier. The band pass filter is composed of R-C components, operational amplifiers and multipliers. The transfer function of the filter can be expressed in Laplace form as the following:

$$\left(\frac{750\ K_{CAS}}{S+50}\right)\left(\frac{18S^2}{(S+6)^2}\right)\left(\frac{14}{S+14}\right)^2\left(\frac{1.56S^2+9.4S+320}{S^2+15.9S+320}\right)\left(\frac{.726S}{S+1}\right)$$

A Bode plot of the filter is shown in Figure 7.

The functions of the band pass filter are:

a. To wash out the steady-state yaw rate signals and to eliminate null offset of sensors.

b. To reduce high frequency signal amplitudes so as to minimize coupling with the higher structural modes.

c. To obtain the proper phasing between yaw rate signal and lower rudder so as to add damping to the aft body lateral flexible modes.

Figure 8 represents the transfer function of yaw rate/lower rudder at BS-2300 whereas Figure 9 shows the effects of the MSAS filter on the above dynamics. The reason for the complexity of the filter is that the 1.8

mode required 'lag' and the 2.4 mode 'lead' in order for the system to add the maximum damping to these modes. Although various body stations were investigated, sensor positions aft of the cg, along the floor 'water line' showed that there was no change in the phase relationship between the 1.8 and 2.4 cps mode.

Figure 10 represents a functional block diagram of the monitoring system and pre-engage mode. The function of the monitor system is the following:

a. Checks the principal gains and phase characteristics of the filter.

b. Detects failure of either gyro.

c. Detects failure of the limiter.

d. Detects failure of gain scheduler.

The purpose of the pre-engage mode is to verify that the MSAS electronic unit, including monitor, is operating correctly.

TEST RESULTS

A system corresponding to the filter shown in Figure 7 was flight tested (no monitor system, etc.). After initial calibration and stability criteria were satisfied (6 db gain margin and 60° phase shift), the system was flown in turbulence. Figure 11 shows one of the many time histories obtained. Figure 12 represents the cumulative accelerations for the time history plots of Figure 11. The MSAS system reduces the aft body flexible mode content by approximately 50% (although Figure 12 shows a 66% reduction). Figure 13 shows the cumulative acceleration at the pilot station. It may be noted that there is very little 1.8 and 2.4 Hz content at the pilot station and very little 4 Hz content in the aft end.

A production type unit has recently been flown (including monitor system, etc.) and the next step will be to certify the system together with the Beta-vane system. The combined systems will then be installed on a production airplane for in-service evaluation.

SECTION II

BETA-VANE SYSTEM

INTRODUCTION

This section discusses a method devised for the 747 airplane of reducing those accelerations due to gust induced rigid airplane motions. As was pointed out in the previous section, the level of RMS accelerations due to turbulence is approximately 50% due to rigid body motions and 50% due to flexible motions (Figure 14). Consequently, a system designed to reduce the rigid body accelerations offers only half the potential reduction in the total level.

SYMBOLS

δ vane rotation

U_B longitudinal body axis velocity

V_B lateral body axis velocity

V_P total velocity

W_B vertical body axis velocity

P_B body axis roll rate

R_B body axis yaw rate

L_1 longitudinal distance from C.G. to vane station

H_1 waterline distance from airplane principal axis to vane station

A_y accelerometer output

Θ pitch angle

Φ roll angle

METHOD OF SOLUTION

The method used for gust alleviation on the 747 in the frequency range 0 - 1 Hz is shown in Figure 15. The basic sensor is a relative wind vane which is used to sense lateral gusts; the output of the vane is used to drive the 747 upper rudder in a sense that reduces the airplane tendency to turn into the gust. The wind vane output signal is composed of the rapid change due to the lateral gust plus changes due to airplane motion from past disturbances. An approximate separation of these signals is accomplished through deriving airplane motion from lateral acceleration, yaw rate and roll attitude as shown in Figure 15. The resulting signal which is proportional to the lateral gust input is put through a band pass filter before being summed with the existing yaw damper signal to drive the upper rudder. The purpose of this filter is to remove steady-state sensor errors and to prevent excitation of the flexible body modes. The approximate location of the wind vane and other system components on the 747 airplane is shown in Figure 16.

ANALYSIS

For the purposes of the analysis, it was assumed that the lateral dynamics could be considered independently and that only lateral gusts were present. The assumed form of these gusts was the typical Von Karman spectrum.

The vane output can be described as:

$$\delta = \frac{GUST}{V_p} + \frac{V_B}{V_p} + \frac{L_1 R_B}{V_p} + \frac{H_1 P_B}{V_p} \qquad (1)$$

where the last three terms give the sideslip angle at the vane location.

To derive a signal proportional to the gust input use is made of a lateral accelerometer mounted at the vane station. The accelerometer output is:

$$A_y = \dot{V}_B + U_B R_B - W_B P_B + L_1 \dot{R}_B + H_1 \dot{P}_B - g \cos\Theta \sin\Phi \qquad (2)$$

consequently,

$$\frac{V_B}{V_p} + \frac{L_1 R_B}{V_p} + \frac{H_1 P_B}{V_p} - \frac{1}{V_p}\int W_B P_B \, dt = \frac{1}{V_p}\int (A_y + g\Phi - V_B R_B)\, dt \qquad (3)$$

or approximately,

$$\frac{V_B}{V_p} + \frac{L_1 R_B}{V_p} + \frac{H_1 P_B}{V_p} \simeq \frac{1}{V_p}\int (A_y + g\Phi - V_p R_B)\, dt \qquad (4)$$

It is therefore possible to rewrite (1) as:

$$\delta - \frac{1}{V_p}\int (A_y + g\Phi - V_p R_B)\, dt = \frac{GUST}{V_p} \qquad (5)$$

all the left side terms of (5) are available and this equation is the basis for mechanization of the system as shown in Figure 15.

The analysis was made using a Boeing derived computer program which accepts matrix inputs. This program provides root locus plots of the system and power spectral densities of designated parameters in response to given forcing functions. The complete analysis included consideration of the lateral airplane dynamics, roll, autopilot, yaw damper and gust suppression system. The performance of the gust suppression system was investigated throughout the flight envelope of the airplane with the intent of determining

optimum system gain for reduction of the rear fuselage lateral acceleration and also to determine system stability. Some particular results of the analysis are shown in Figure 17. Figure 17 shows a root locus plot for different gains of the gust suppression system with the corresponding RMS 'g' levels at an aft body station shown in Figure 18. It can be seen that a reduction of about 30% in the RMS 'g' level can be obtained at the bucket of the curve shown in Figure 18. This particular gain affects the airplane stability very slightly as can be seen in Figure 17. Similar results were obtained for various airplane altitudes and speeds, the value of gust suppression gain remaining essentially the same for minimum 'g' levels.

The reason for the change in airplane stability is the approximate form adopted for compensating the vane output for airplane motion. Theoretically, this signal could be perfect, in which case, the root locus shown in Figure 19 results for all system gains. The approximate method of compensation was chosen for practical implementation.

TEST RESULTS

A system corresponding to that shown in Figure 15 was constructed and test flown in the 747 airplane. Initial flights were made to calibrate the wind vane sensor and to investigate airplane handling with the system engaged in calm air. Pilot comments were that the operation of the system had undetectable effect on handling characteristics in either normal or emergency maneuvers. Subsequently, several flights to investigate performance during turbulence were made. Typical data from one such flight is shown in Figures 20 and 21. Figure 20 shows a typical gust signal command measured at the input to the Beta filter summing amplifier while Figure 21 shows the RMS 'g' levels recorded at the aft body station with the system ON then OFF in sequence. The reduction in acceleration levels with the system ON is of the same magnitude as that predicted.

SERVICE EVALUATION

To obtain more data on the system, it has been installed on a commercial carrier airplane with a limited instrumentation package. Because this installation operates at a reduced gain while information is being collected, the results do not show such a large reduction in acceleration levels as those obtained during Boeing tests. A typical example of some of this data is shown in Figure 22, where a comparison of the acceleration levels at an aft body station during turbulence is shown with the system ON and OFF.

CONCLUSION

The development and testing of the Beta-vane and MSAS systems have been described. Data from flight test have indicated that a 50-70 percent reduction in aft body lateral acceleration levels can be achieved with the above systems. Non-linear filtering and different sensors will be the subject of future research.

REFERENCES

1. E. C. Levy, "Complex Curve Fitting," IEEE Transactions on Automatic Control, vol AC-4, pp 37-44; May 1959.

2. C. K. Sanathanan and J. Koerner, "Transfer Function Synthesis as a Ratio of Two Complex Polynomeals," IEEE Transactions on Automatic Control, pp 56-58; Jan 1963.

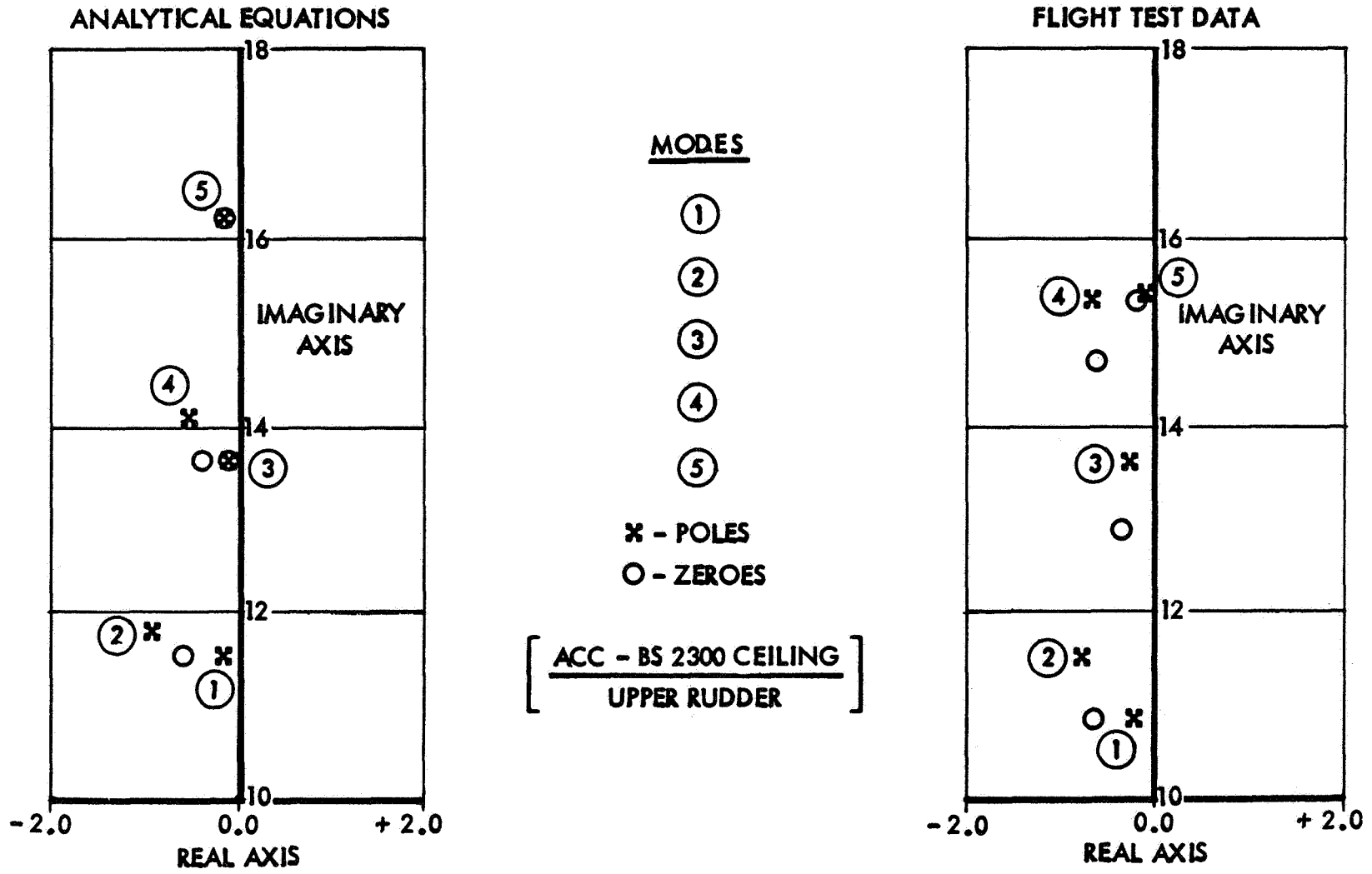

COMPARISON OF ANALYTICAL AND FLIGHT TEST DATA

FIGURE 1

C 5

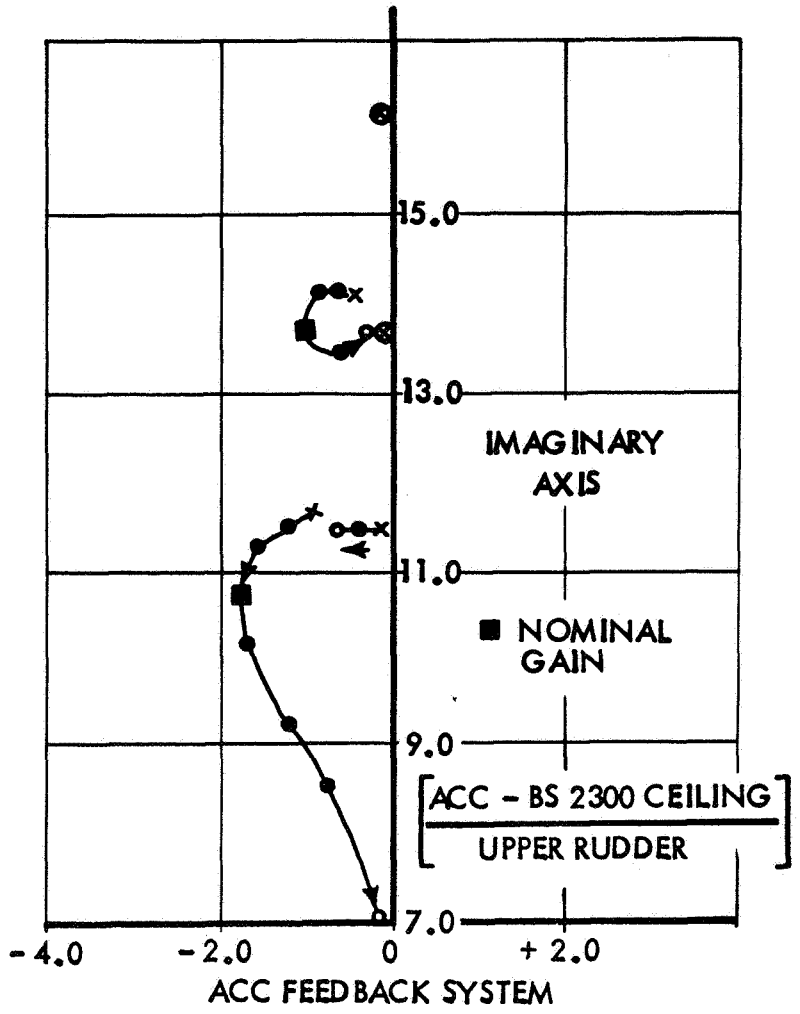

ROOT LOCUS PLOT OF CONTROL SYSTEM BASED ON ANALYTICAL EQUATIONS

FIGURE 2

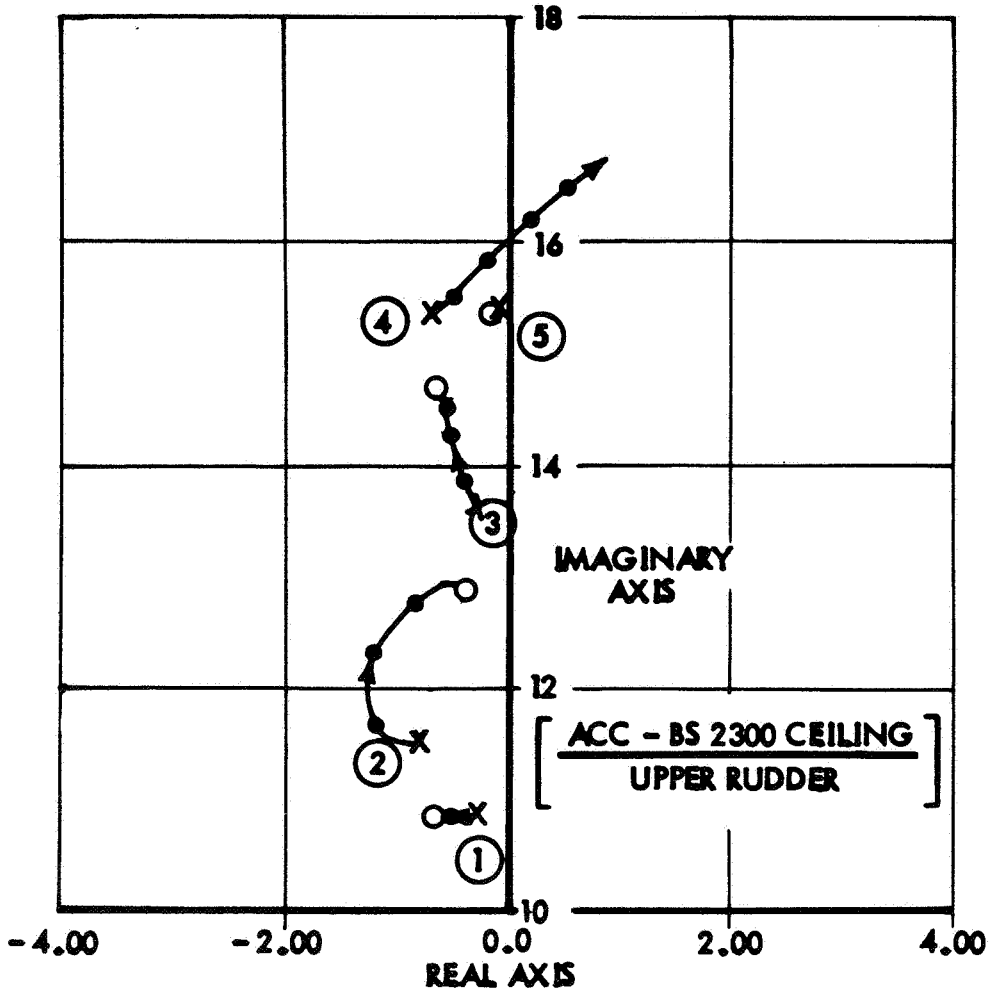

ROOT LOCUS OF PLOT CONTROL SYSTEM BASED ON CURVE FIT COMPUTER PROGRAM

FIGURE 3

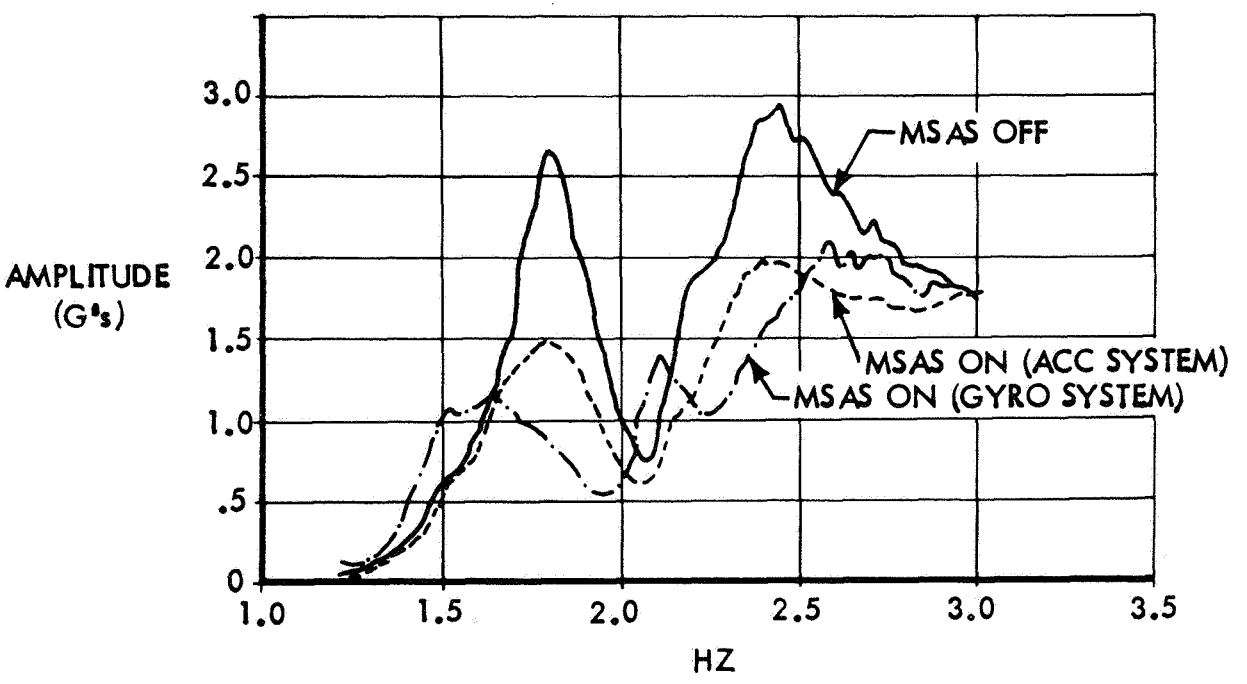

TRANSFER FUNCTION

LATERAL ACCELERATION (AFT BODY)
RUDDER (LOWER)

- **ALTITUDE = 31,000 FT**
- **MACH = .86**

FIGURE 4

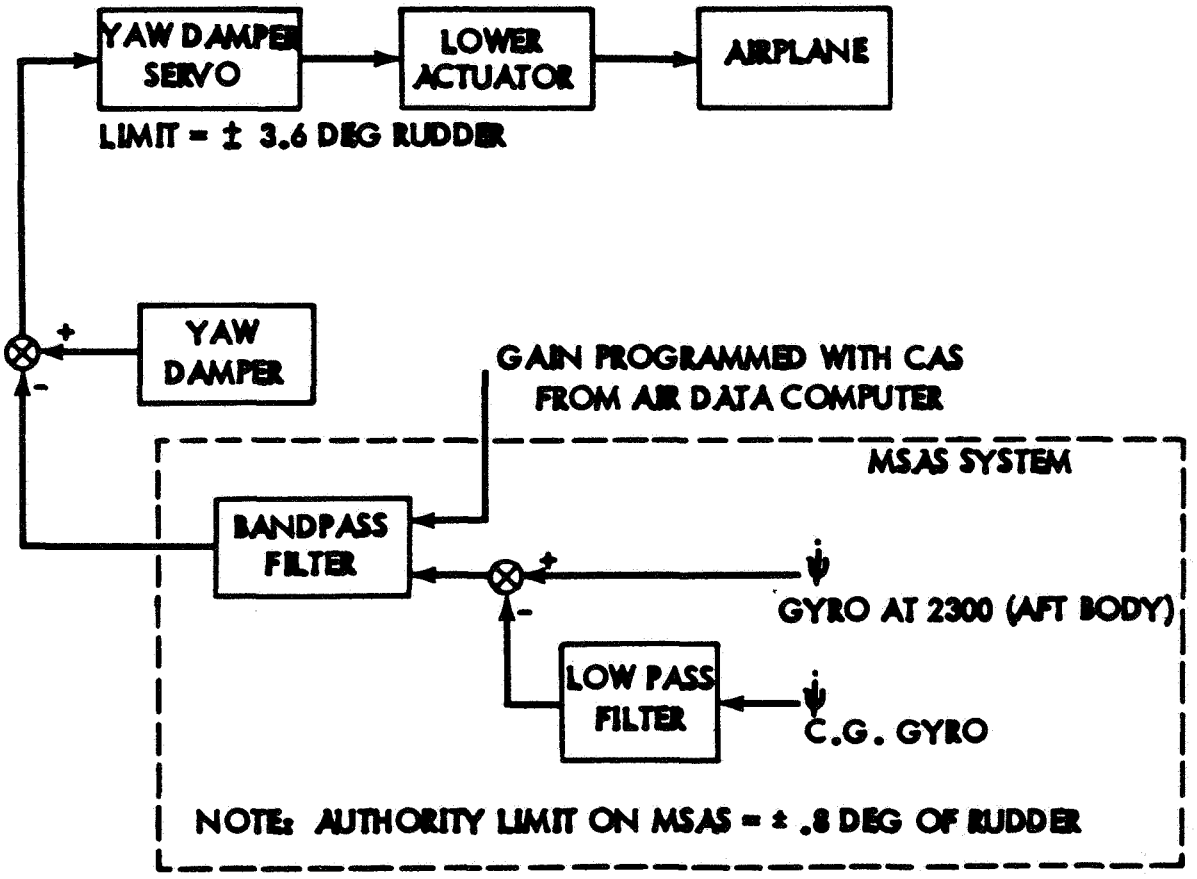

BLOCK DIAGRAM OF MSAS CONTROL SYSTEM

FIGURE 5

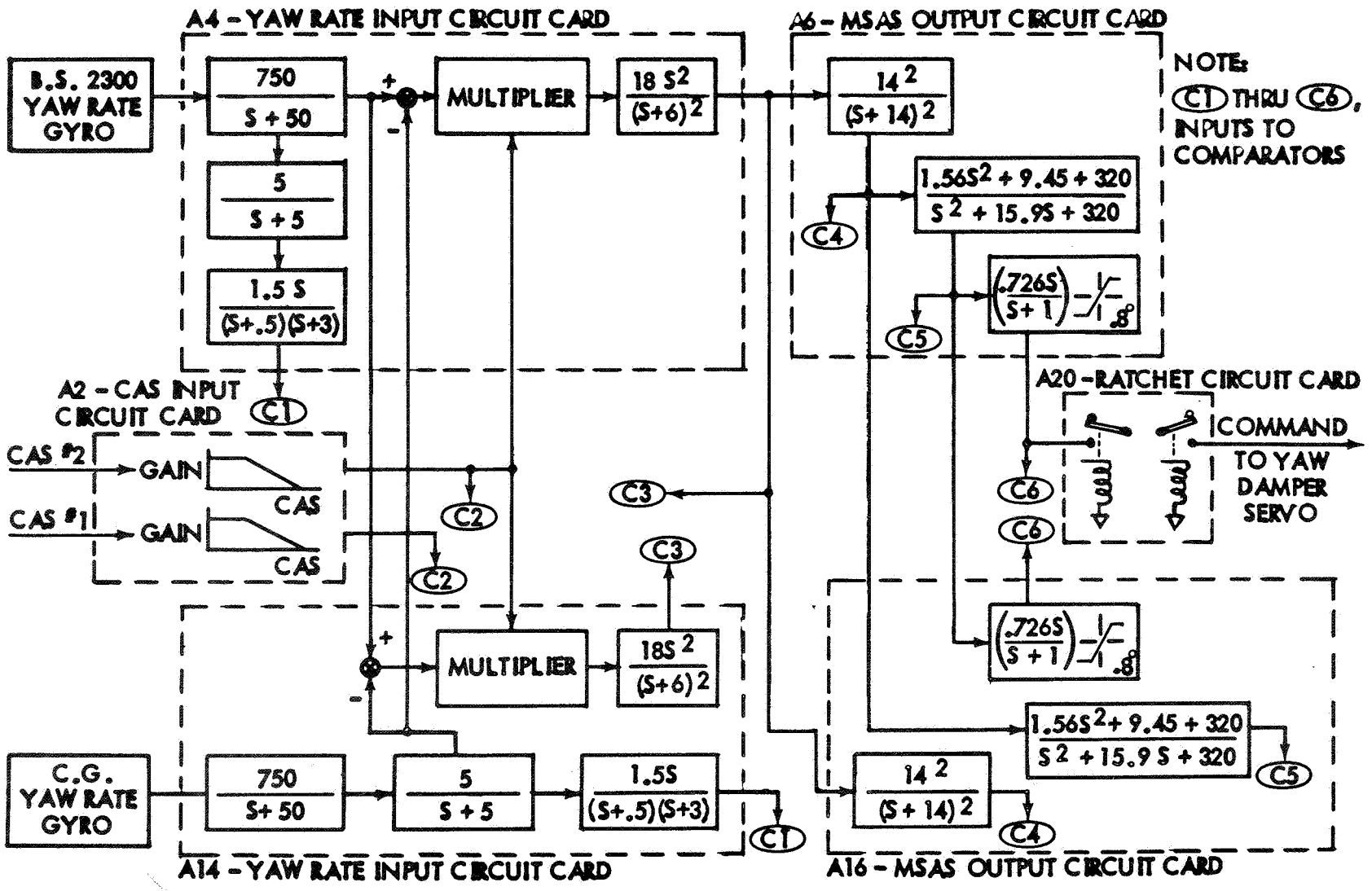

SYSTEM DIAGRAM MODAL SUPPRESSION AUGMENTATION SYSTEM

FIGURE 6

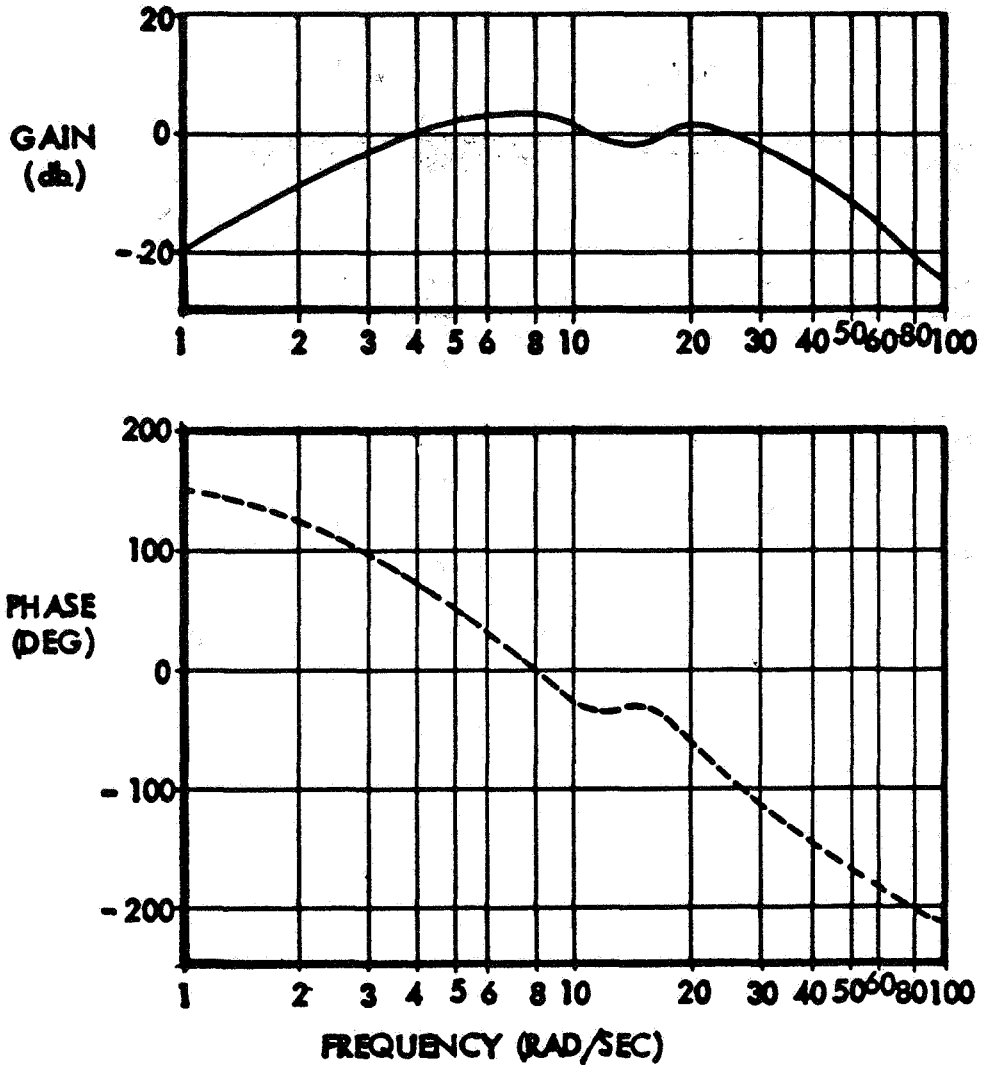

GAIN AND PHASE PLOT OF MSAS FILTER

FIGURE 7

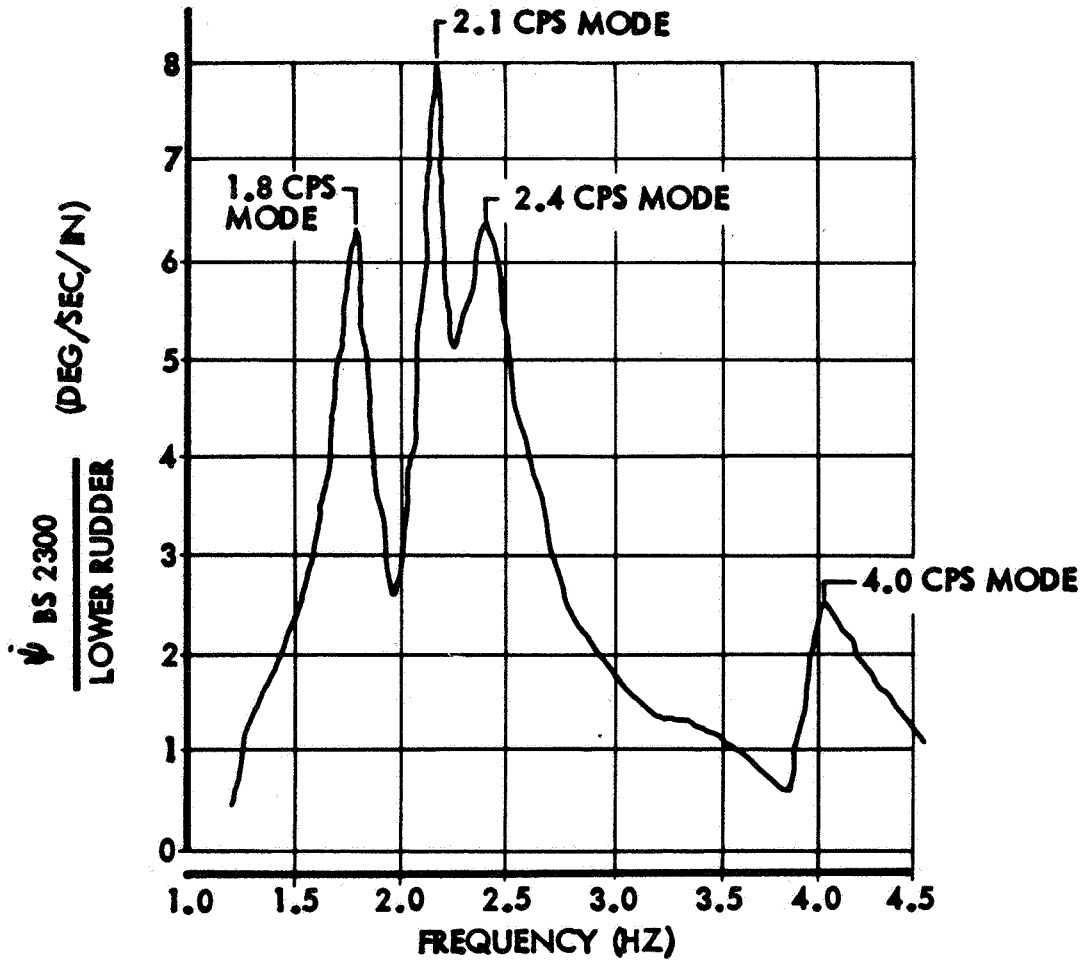

AMPLITUDE RESPONSE - $\dot{\psi}_{BS\ 2300}$ / LOWER RUDDER INPUT

FIGURE 8

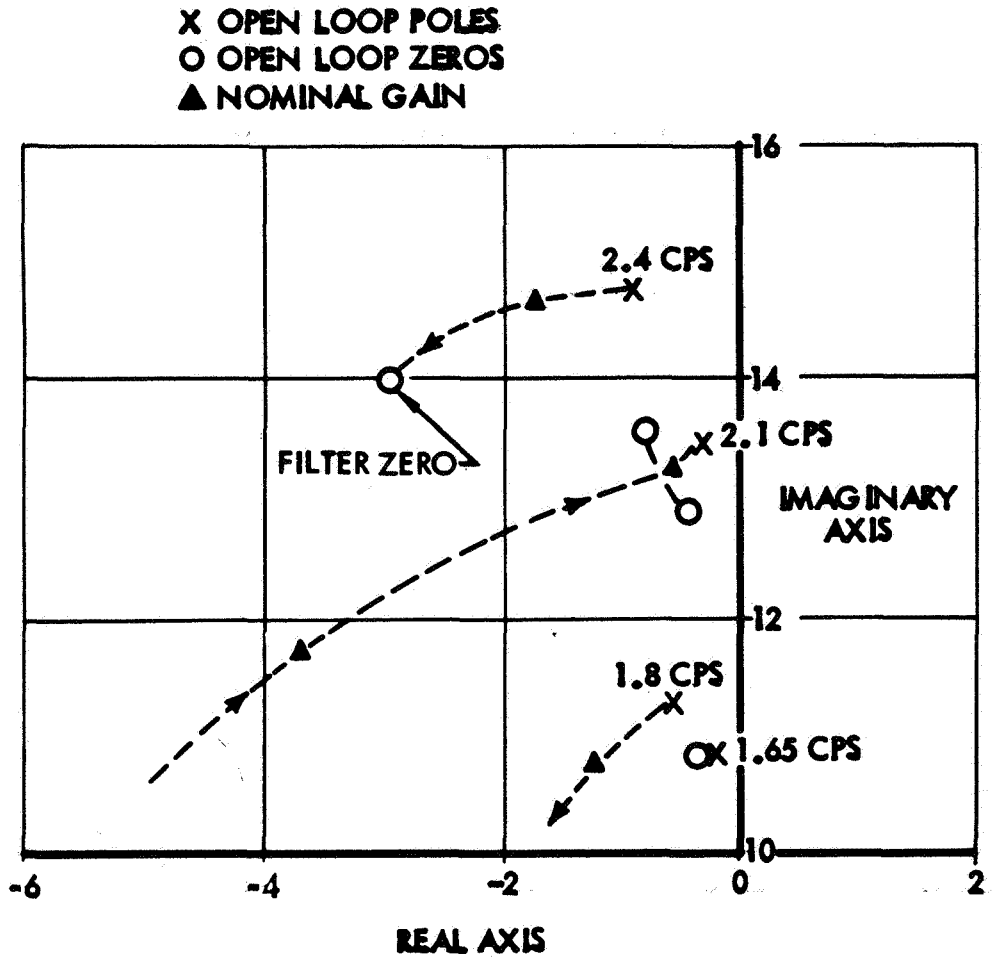

ROOT LOCUS PLOT OF CONTROL SYSTEM

FIGURE 9

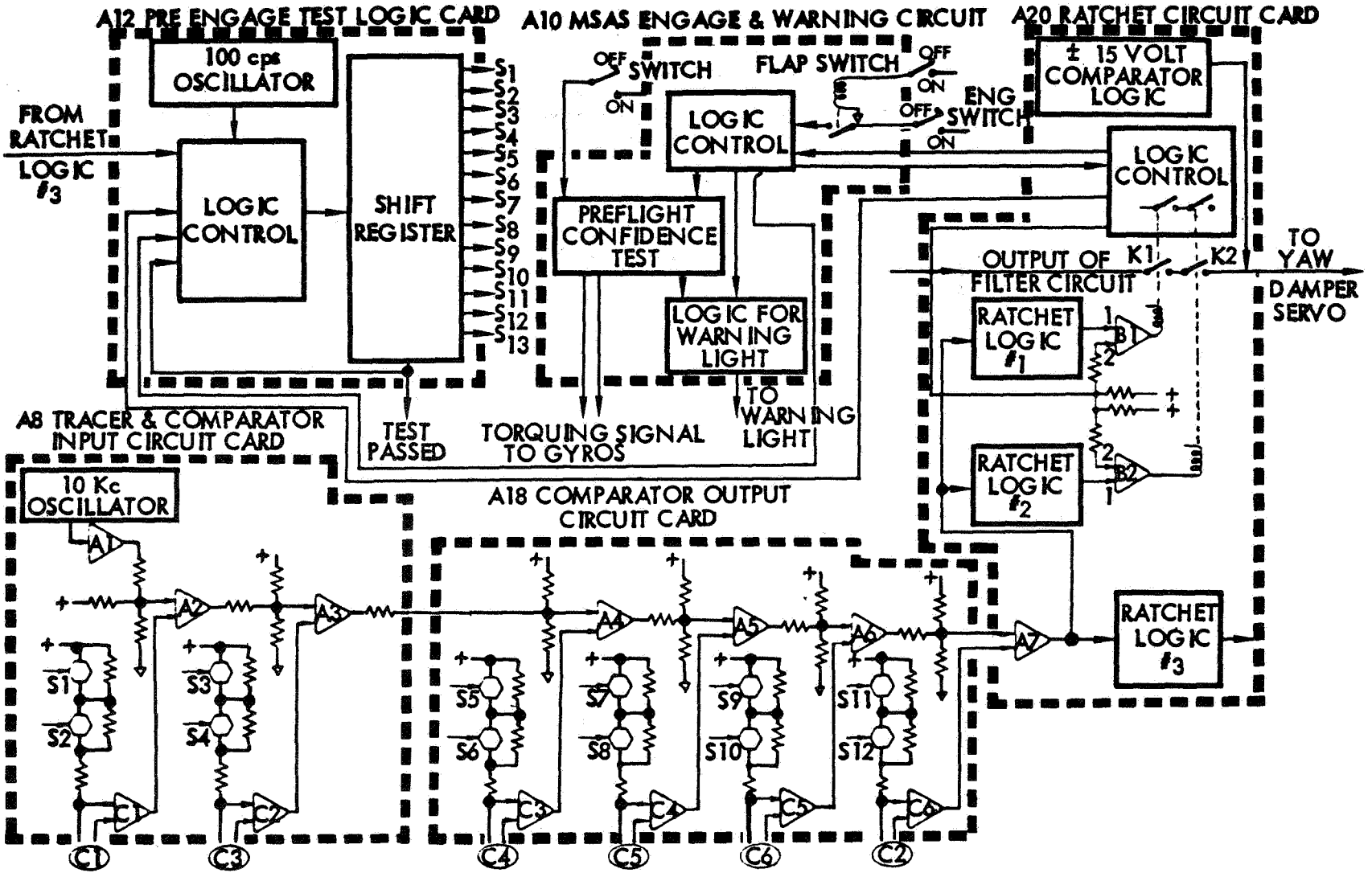

FUNCTIONAL BLOCK DIAGRAM OF MSAS MONITORING SYSTEM

FIGURE 10

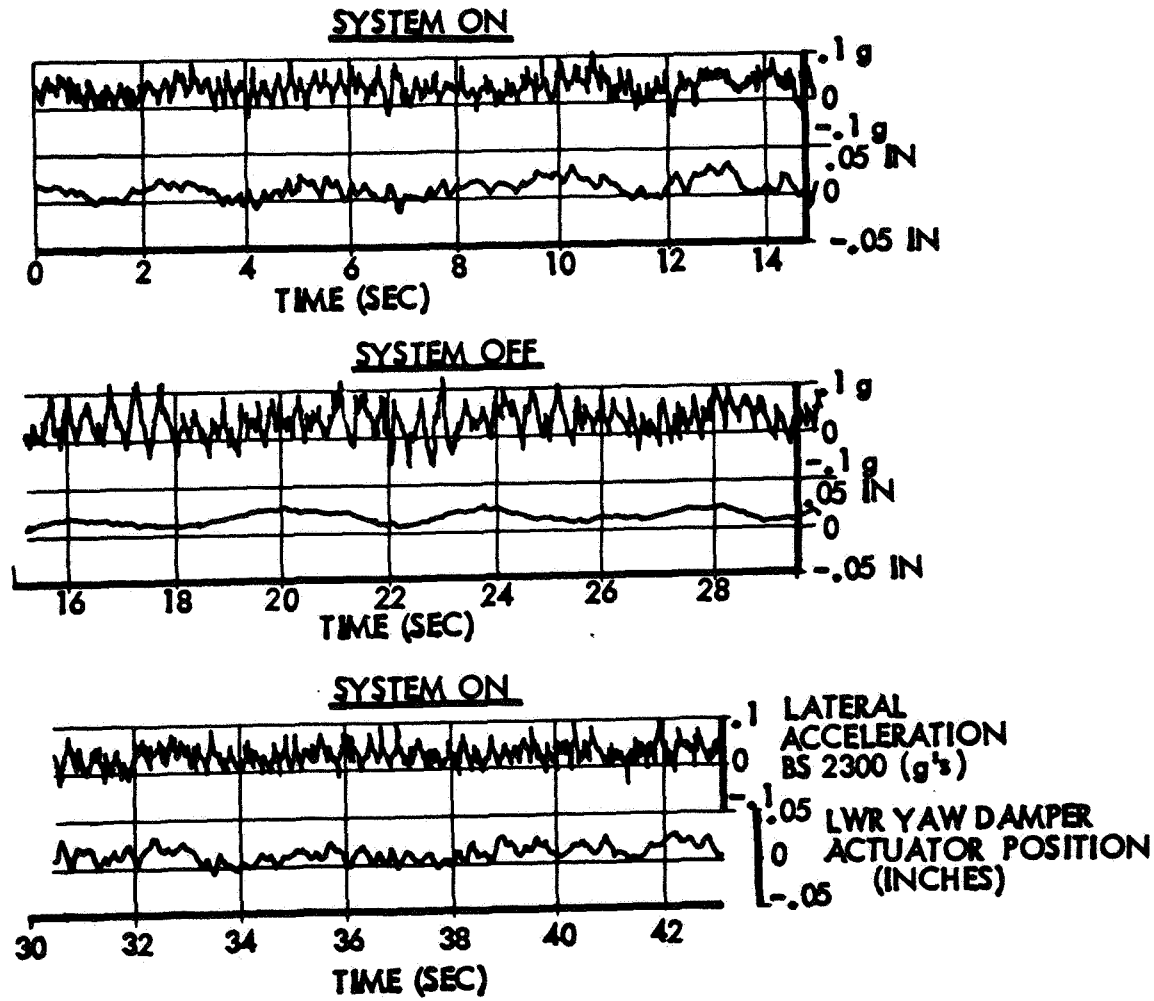

AIRPLANE RESPONSE IN TURBULENCE WITH AND WITHOUT MSAS

FIGURE 11

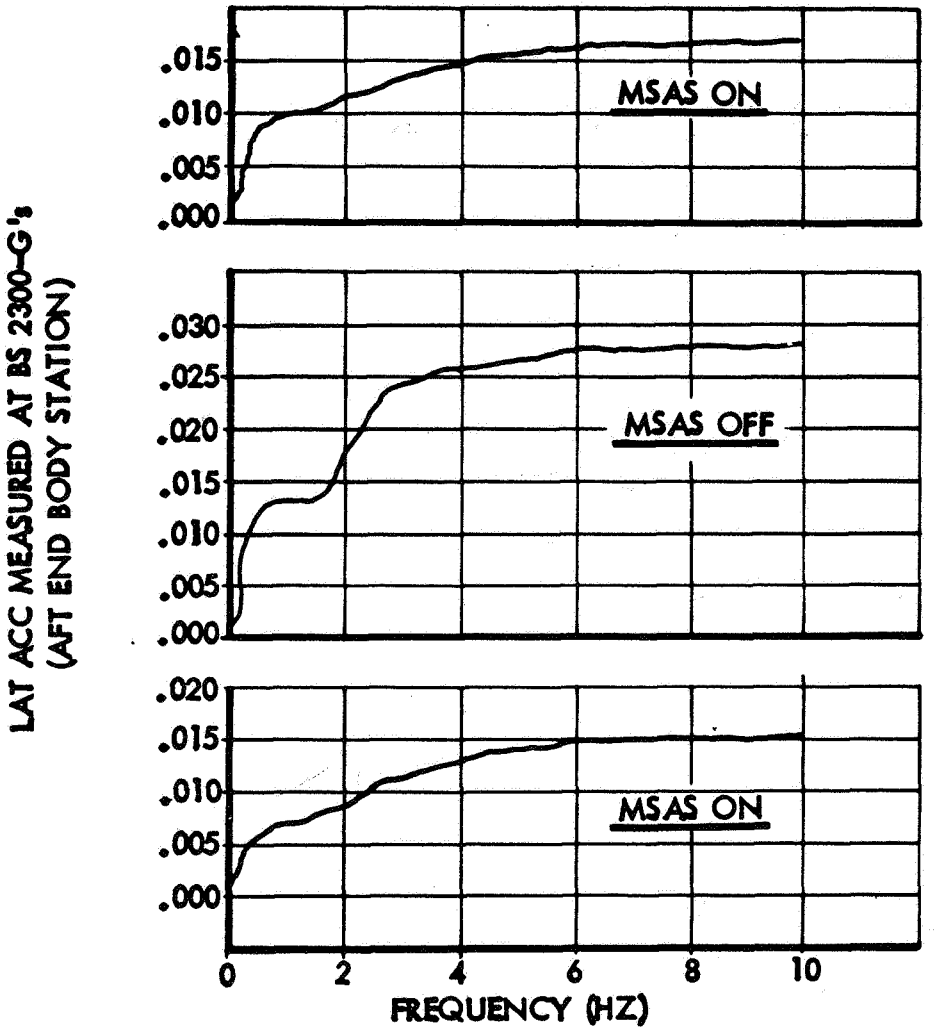

ACCUMULATIVE RMS - TURBULENCE

FIGURE 12

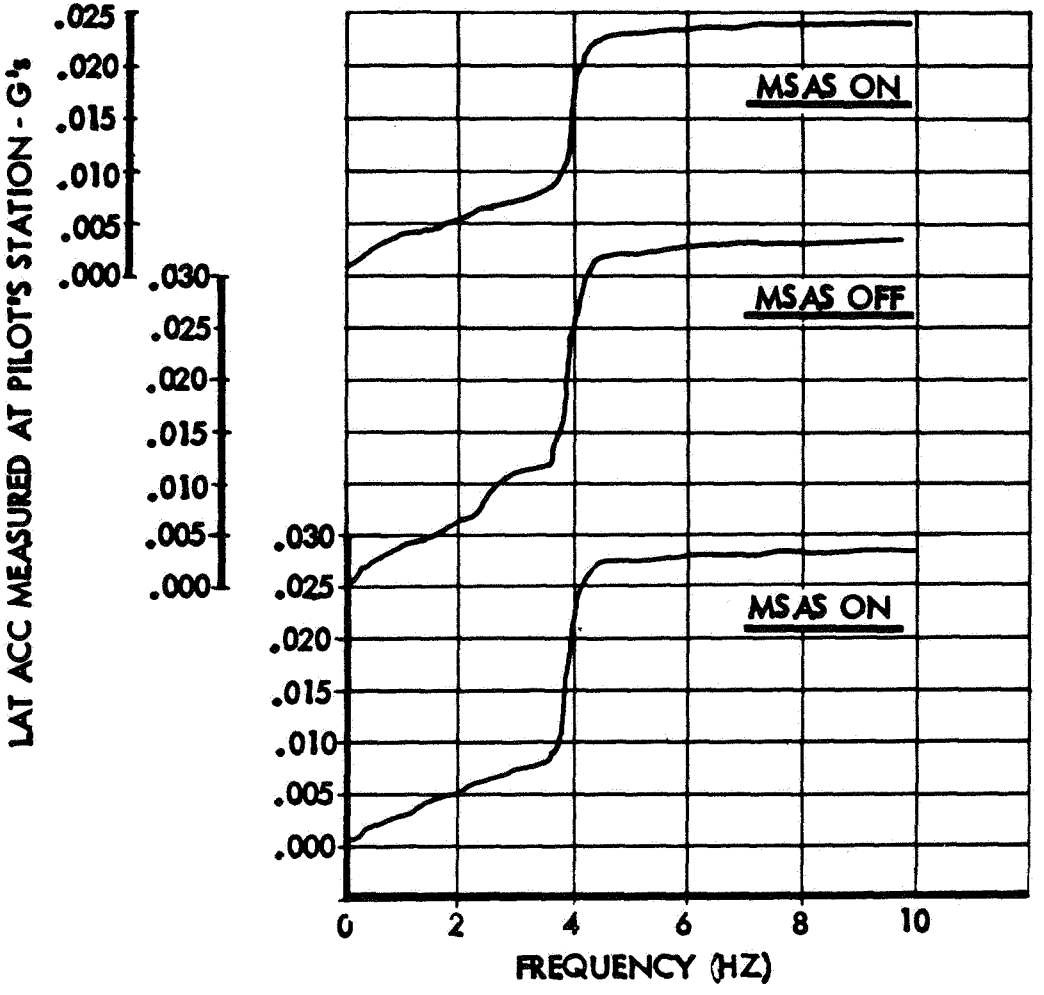

ACCUMULATIVE RMS - TURBULENCE

FIGURE 13

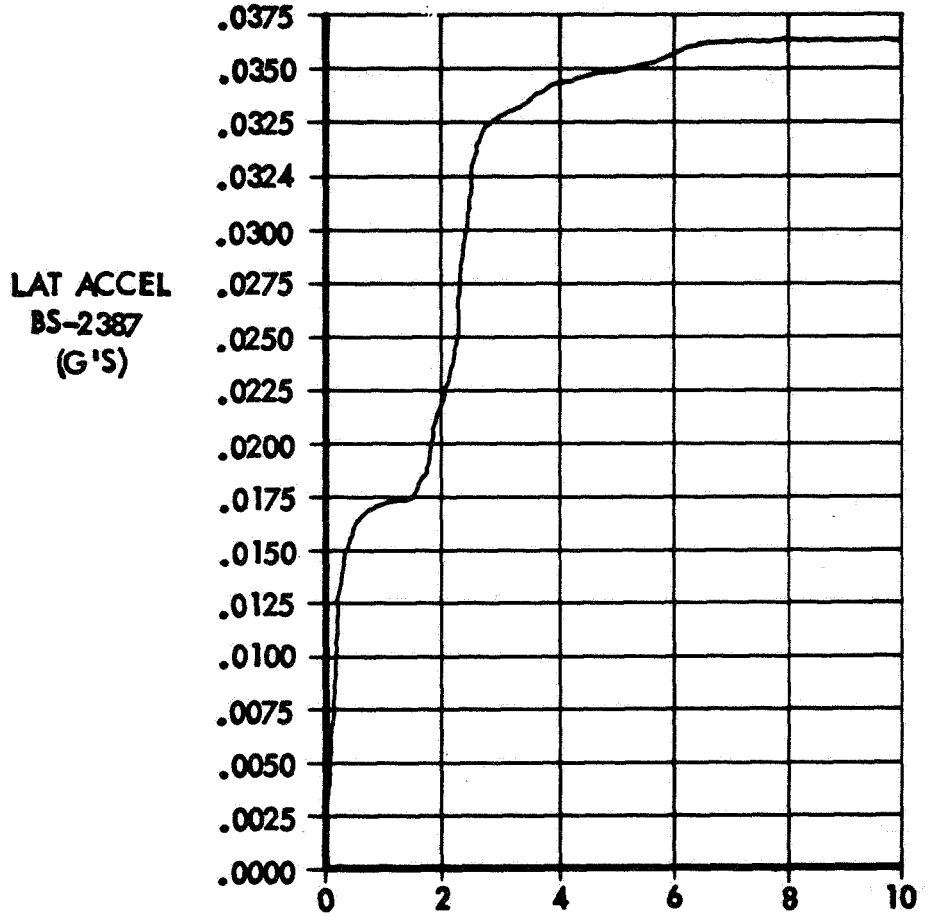

CUMULATIVE RMS - QANTAS BETA

SYSTEM EVALUATION IN TURBULENCE

FIGURE 14

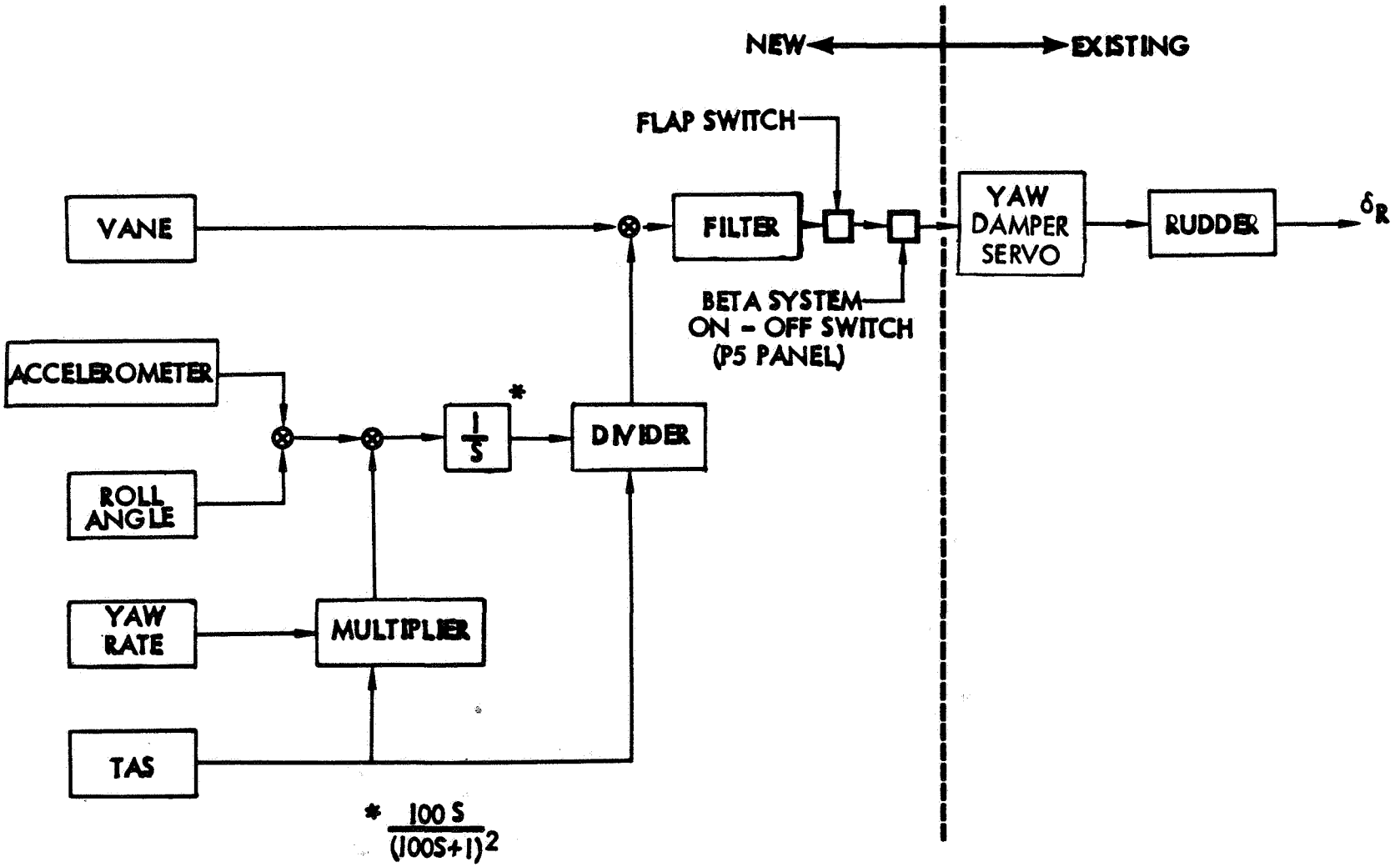

BETA MODIFIED YAW DAMPER BLOCK DIAGRAM

FIGURE 15

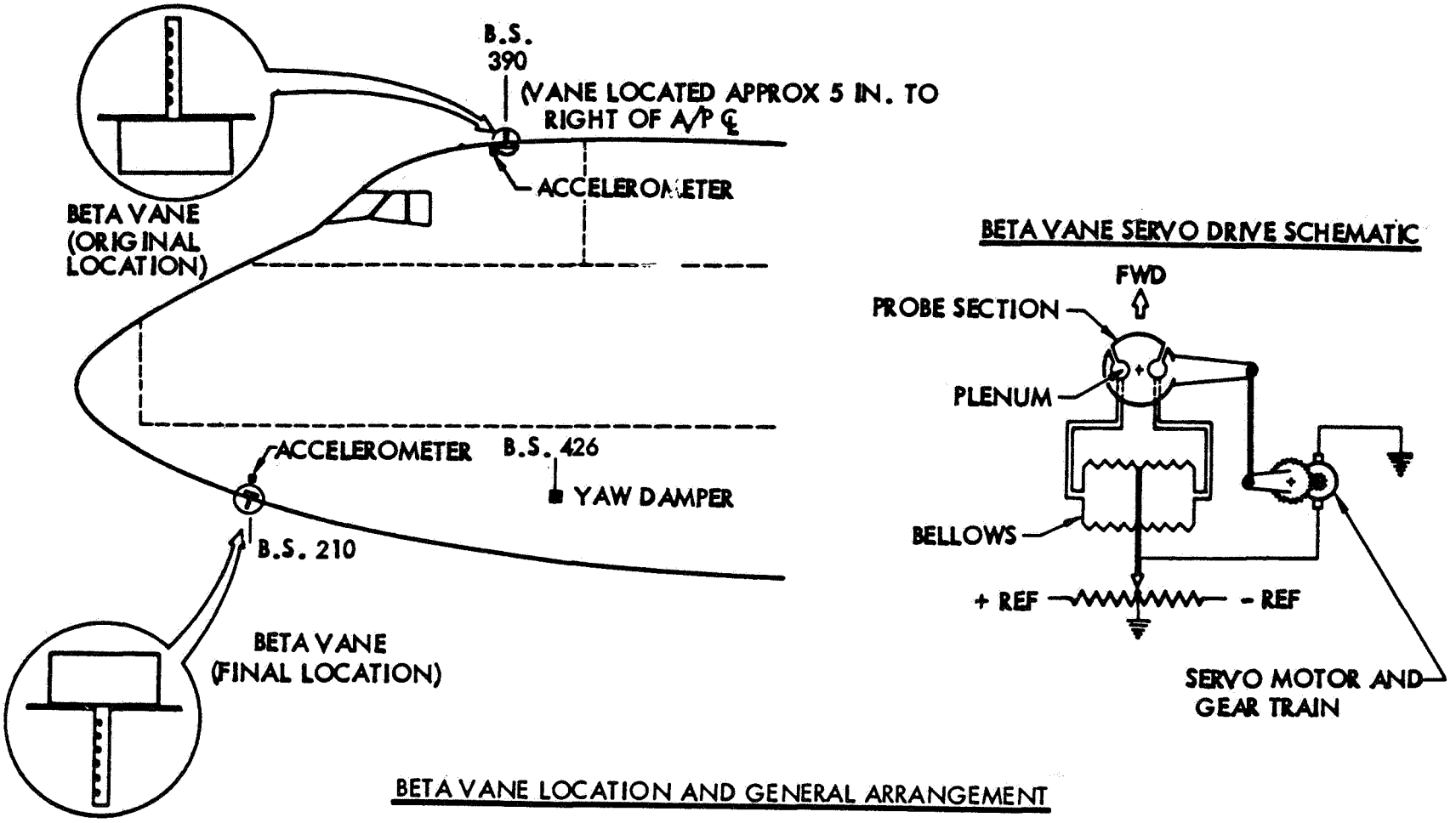

BETA VANE LOCATION AND GENERAL ARRANGEMENT

FIGURE 16

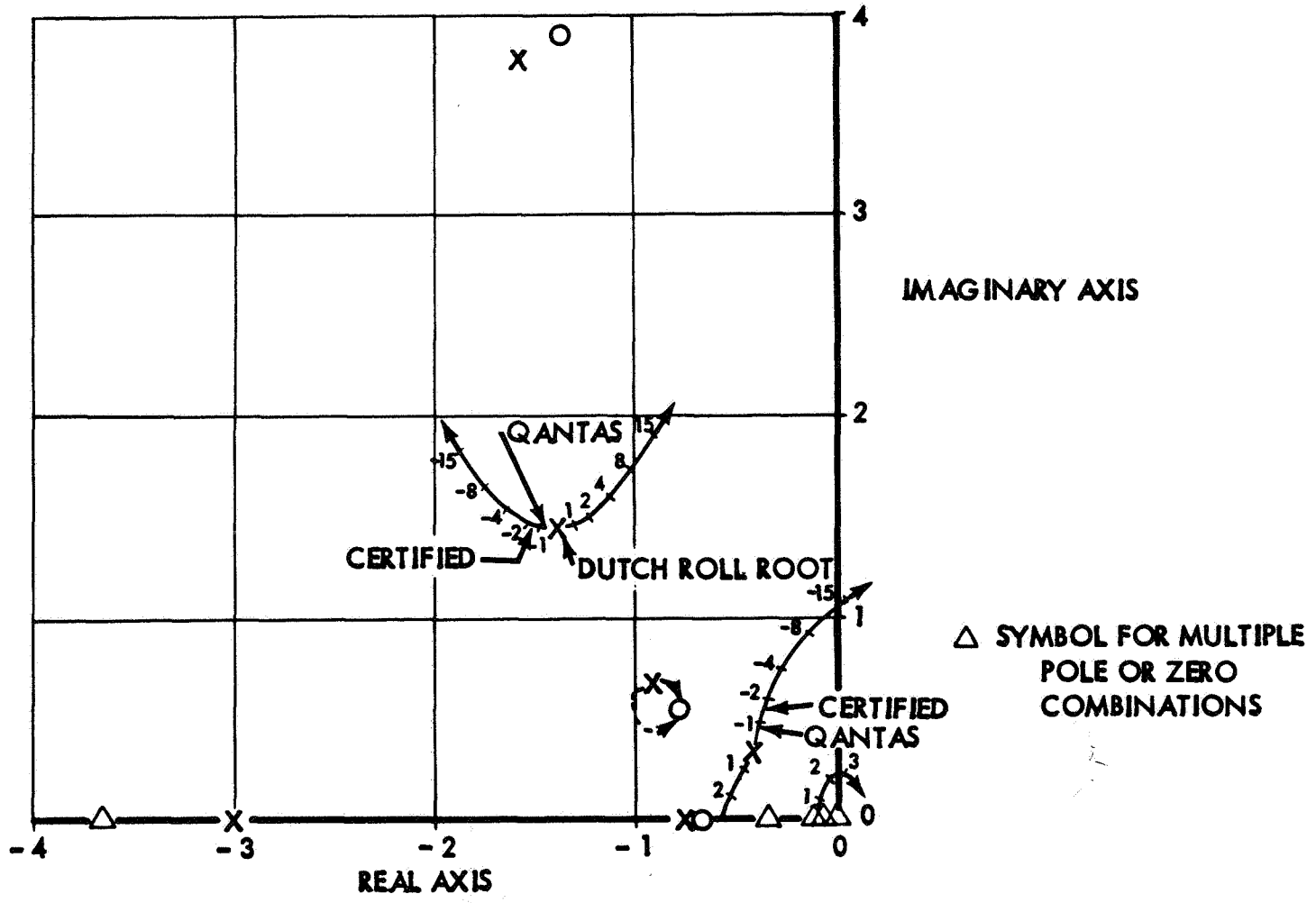

ROOT LOCUS FOR PARTIALLY COMPENSATED SYSTEM WITH NOMINAL YAW DAMPER GAIN

FIGURE 17

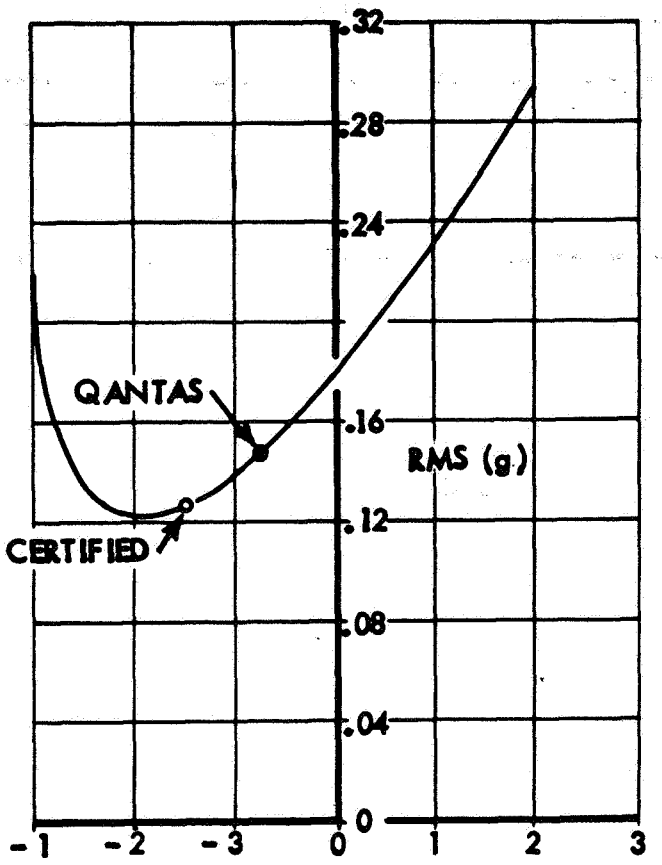

CUMULATIVE ROOT MEAN SQUARE ACCELERATION (BS 2300) VERSUS SYSTEM GAIN

Actual Compensation (Beta System)

FIGURE 18

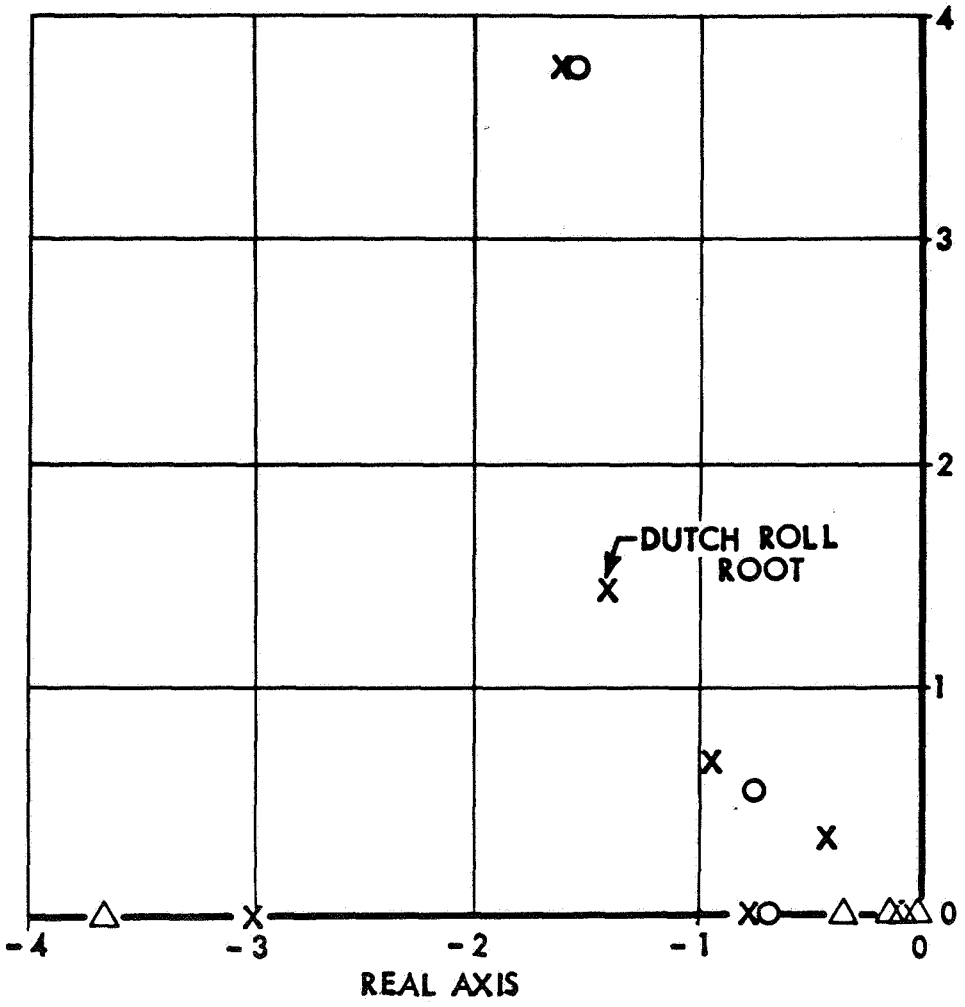

IMAGINARY AXIS

△ SYMBOL FOR MULTIPLE POLE OR ZERO COMBINATIONS

ROOT LOCUS FOR PERFECTLY COMPENSATED SYSTEM

Reduced to Airplane Roots Only

FIGURE 19

POWER SPECTRUM OF COMPENSATED BETA SIGNAL MEASURED IN TURBULENCE

FIGURE 20

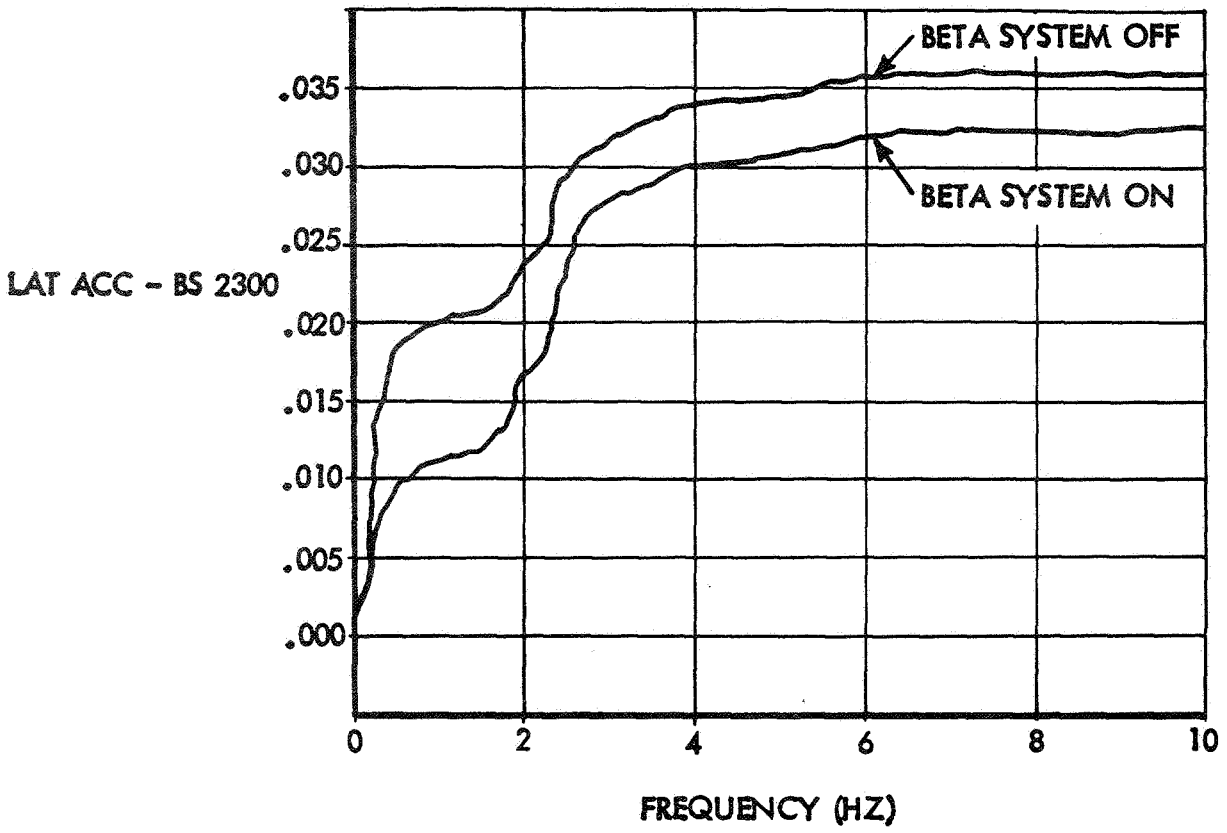

CUMULATIVE RMS

Beta System In Turbulence

FIGURE 21

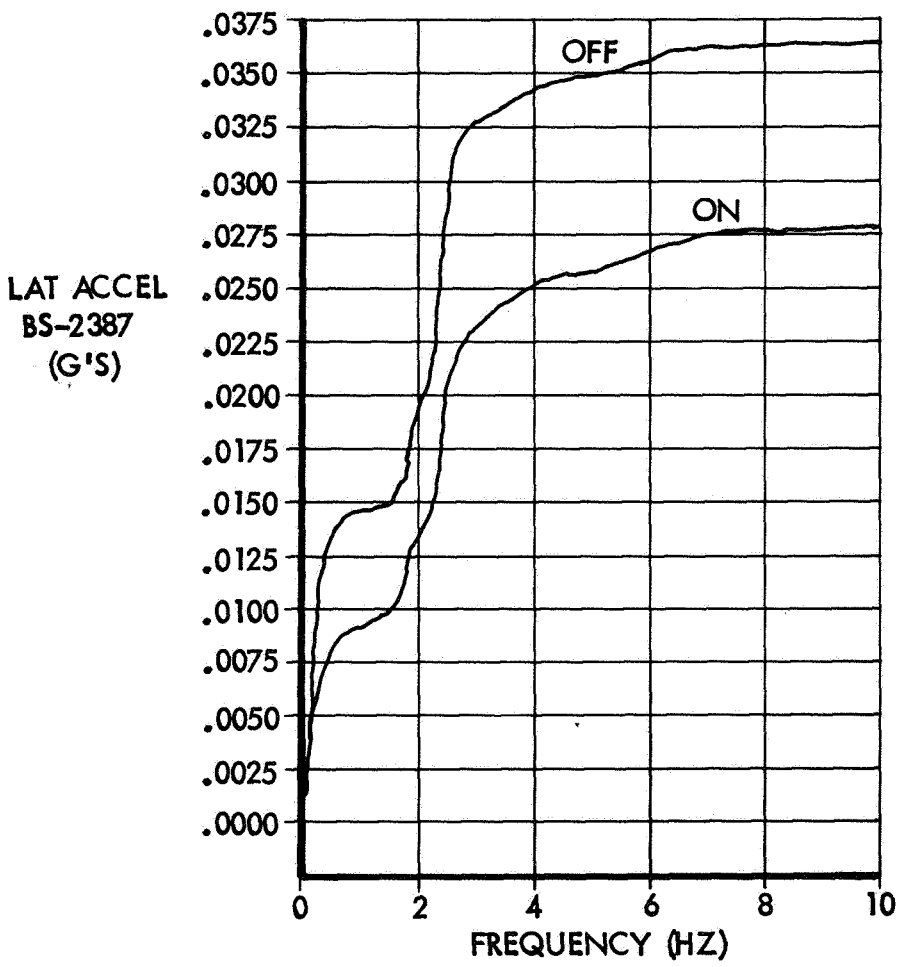

CUMULATIVE RMS QANTAS BETA
SYSTEM EVALUATION IN TURBULENCE

FIGURE 22